Mansoura Engineering Journal

Volume 31 | Issue 1 Article 13

12-12-2020

Dispersion Effect on the Performance of FO-CDMA Passive Correlator Receiver.

Kamel Hassan
Electrical Engineering & Computers Dept., Higher Technological Institue, 10th of Ramadan city, Egypt,

Atef Ghuniem
Electrical Engineering Dept., Faculty of Engineering in Port Said, Suez Canal University, Egypt.

Asmaa Abd Elftah
Electrical Engineering Dept., Faculty of Engineering in Port Said, Suez Canal University, Egypt.

Recommended Citation

Hassan, Kamel; Ghuniem, Atef; and Abd Elftah, Asmaa (2020) "Dispersion Effect on the Performance of FO-CDMA Passive Correlator Receiver.," *Mansoura Engineering Journal*: Vol. 31 : Iss. 1 , Article 13.
Available at: https://doi.org/10.21608/bfemu.2020.129245

DISPERSION EFFECT ON THE PERFORMANCE OF FO-CDMA PASSIVE CORRELATOR RECEIVER

تأثير التشتت اللوني على أداء أحد مستقبلات ألياف الاتصال الضونية ذو التقسيم متعدد الشفرات و هو مستقبل الربط السلبي

Kamel Hassan, SM, IEEE[1], Atef Ghuniem[2], and Asmaa Abd Elftah[2]

الخلاصه باللغه العربيه:

في هذا البحث يتم دراسة تأثير التشتت اللوني على أداء أحد مستقبلات ألياف الاتصال الضونية ذو التقسيم متعدد الشفرات و هو مستقبل الربط السلبي. و يتم استخدام الشفرات الضونية المتعامدة. و قد تم أخذ تأثير جميع مصادر الضوضاء في الاعتبار. وقد تم استنتاج صورة تقريبية لمعدل الخطأ في النظام المستخدم في حالة استخدام ثلاثة أنواع مختلفة من الألياف الضونية و هي SMF، DSF و DCF مع افتراض أن النبضات المرسلة لها شكل Gaussian. و قد أوضحت النتائج أن تأثير التشتت يزيد مع زيادة طول الشفرة بينما زيادة وزن الشفرة يقلل من تأثير التشتت فقط عندما تكون قدرة الاشاره أقل من حد معين.

ABSTRACT

In this paper the effect of chromatic dispersion on the performance of fiber-optic-code-division-multiple-access (FO-CDMA) passive correlator receiver has been investigated. Optical orthogonal codes (OOCs) are utilized as signature sequences. The effect of all major noise sources (quantum shot noise, dark current noise, and Gaussian circuit noise) has been taken into-consideration. We have derived an approximate analytical expression for the bit error rate (BER) of the system. BER analysis of the system is performed in the case of three different fiber types which are 1) a standard single mode fiber (SMF), 2) a dispersion shifted fiber (DSF), and 3) a fully dispersion compensated fiber (DCF) assuming a Gaussian pulse shape for the transmitted pulses. The dispersion effect has been checked for different system parameters. The numerical results demonstrate that for a fixed number of simultaneous users "N" ,the dispersion effect increases with increasing the code length "F" .It is found also that increasing code weight "k" leads to minimize the dispersion effect in the standard SMF as long as the power level is kept less than a pre-determined value.

KEYWORDS: Chromatic dispersion, Passive correlator receiver, FO-CDMA.

[1] Electrical Engineering & Computers Dept., Higher Technological Institute, 10th of Ramadan city, Egypt.

[2] Electrical Engineering Dept., Faculty of Engineering in Port Said, Suez Canal University, Egypt.

Accepted March 8, 2006

1. INTRODUCTION

Optical access networks have been considered as very attractive infrastructures to satisfy the increasing traffic demands. Up to now, various types of structures and techniques have been proposed based on time division multiple access (TDMA) or wavelength division multiple access (WDMA). However, due to their inherent structure; the cost per user is quite so high that alternative approaches for high-speed access network with low cost need to be investigated. The optical CDMA (O-CDMA) system is a promising candidate for achieving this objective [1]. This system depends on assigning individual codes to each user at the transmitter and the received signals are decoded using the matched codes at the receiver [2], [3].

The effect of chromatic dispersion, which results in temporal widening of optical pulses, is more sever for O-CDMA systems than other optical systems since the chip duration in O-CDMA system is ultrashort even though the transmitted bit rate is moderate. This is due to high processing gain of the system. Dispersion penalty for 1.3-μm lightwave system is analyzed in [4] without taking into account receiver details, the dispersion penalty is simply obtained by comparing the received power with and without dispersion effect at the decision point which assumed to be located at the pulse center. The effect of chromatic dispersion on multi-wavelength optical CDMA (MW-O-CDMA) systems is explored in [5] through simulation of realistic networks. The performance of an asynchronous phase-encoded O-CDMA system is evaluated in a dispersive fiber medium in [6]. BER analysis of the system is performed in the case of ordinary SMF, dispersion shifted fiber (DSF), and a fully dispersion compensated fiber (DCF) assuming a Gaussian pulse shape for the pulse generator.

Performance analysis of the passive correlator receiver was the subject of many articles [7], [8], [9]. In [7], the performance is analyzed taking into consideration only the effects of the multiple access interference [MAI]. In [8] and [9], the effects of all receiver

noise sources have been considered, whereas the effects of chromatic dispersion have been neglected.

In this paper we study the effect of chromatic dispersion on the performance of an O-CDMA receiver, namely, passive correlator receiver. Optical orthogonal codes (OOCs) are utilized as signature sequences. The effect of all major noise sources, i.e. quantum shot noise, dark current noise, and Gaussian circuit noise has been taken into consideration. Fiber nonlinearities are assumed to be suppressed through this analysis using the technique proposed in [10] which makes use of fiber Bragg grating (FBG) designed such that it is transparent to the forward-propagating optical pulses but the spectrum of the Stokes pulse generated through SBS falls entirely within its stop band. As a result, any stokes radiation in the backward direction will be reflected by the FBG and propagates in the forward direction. The loss in fiber is not taken into-consideration. The reduction in the power level will be due to the dispersion effect only.

The rest of the paper is organized as follows; section 2 gives a description of fiber-optic CDMA network and the passive correlator receiver structure. In section 3, we present bit error rate (BER) analysis of passive correlation receiver. In section 4, the numerical results using computer simulation are shown. Finally the conclusions are given.

2. FIBER-OPTIC CDMA NETWORK

A typical structure of a FO-CDMA network is shown in Fig.1. In transmission side there are N_{max} different transmitters connected to star coupler (N_{max}x1) transmission channel which is typically SMF. In receiving side a star coupler (1xN_{max}) is coupled to N_{max} different receivers, where N_{max} represents the size of the star coupler, i.e., N_{max} is the maximum number of allowed users.

Each information source provides an information bit for a laser based optical on-off keying (OOK) modulator every T second.

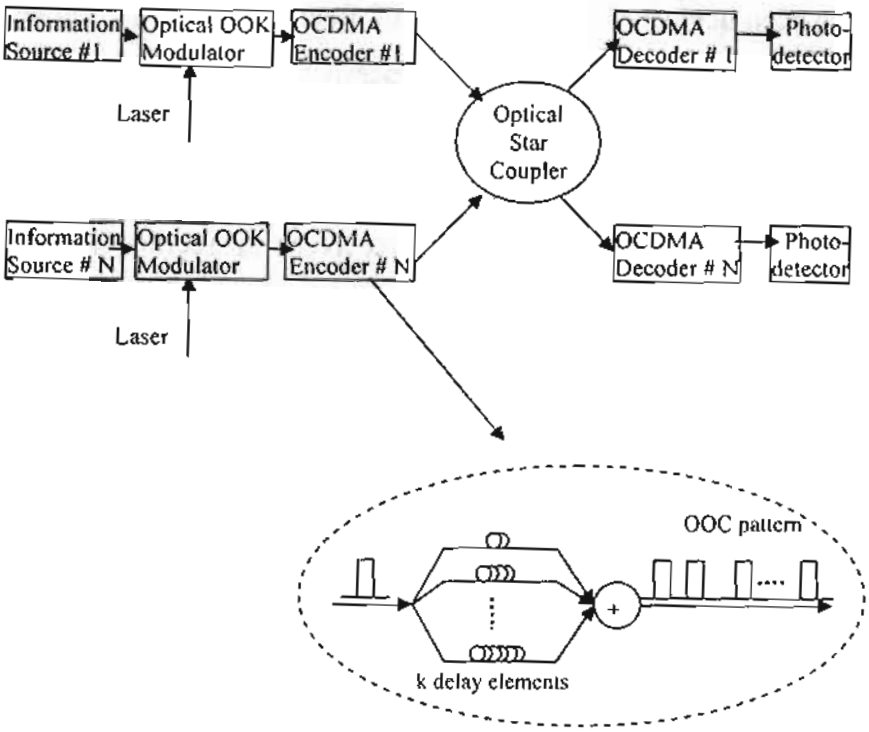

Fig.1. Structure of a typical OCDMA network

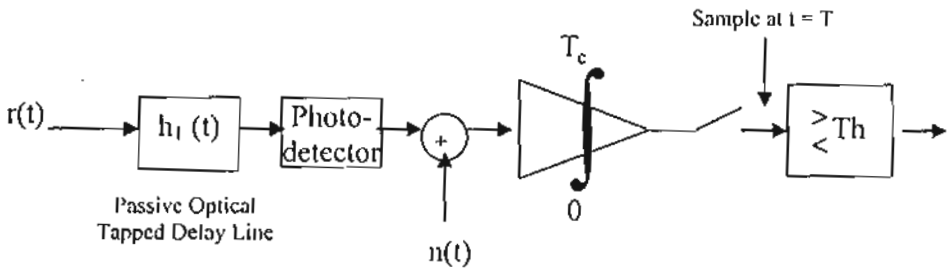

Fig.2. Passive correlator receiver.

The external modulator turns the light of the continuous wave (CW) laser on and off based on the data and then generates a narrow pulse (chip) with duration T_c=T/F where F is the CDMA code length. In an optical CDMA encoder, energy of pulses generated by data modulator is split into k (code weight) equal parts. Each part undergoes a pre-specified delay and then recombines in such a way to form the CDMA code pattern. This process is usually performed using optical coupler and optical tapped delay lines [11]. We assume that OOC with minimum auto and cross-correlation is assigned to each user's encoder, i.e., an (F, k, 1) OOC with N_{max} codewords is used [12]. The construction of such codes was the subject of many articles [12], [13]. The output of each encoder is then coupled into SMF through a star coupler. At the receiver, a copy of the desired signal along with the interference from all N-1 active users will be received, and the receiver should be able to decide which bit of the desired user has been sent. BER performance of the receiver is highly affected by the architecture of CDMA decoder. The structure of the passive correlator receiver is shown in Fig.2. In this receiver, the incoming signal is divided into k equal parts; each part undergoes a time delay complement to one of delay elements of CDMA encoder. For example, if F=32 and the transmitter sequence is (1, 4, 13, 30), then the delay elements will be designed to generate delays ($31T_c$, $28T_c$, $19T_c$, $2T_c$). Output of these k delay lines will be combined to produce a single high chip level at the end of the bit duration. Then this optical signal is applied to a photodetector to be converted into an electrical signal. Integrating this signal, the output voltage will be sampled at the end of each bit interval and then will be compared against a threshold level "v_{Th}". Finally an estimate of the transmitted bit will be given.

The use of a chip time integrator has an advantage of reducing the contribution of dark current noise and Gaussian noise. However, since the integration time is small, the receiver needs a very high-speed electronic circuitry which should operate at chip-rate speed ($1/T_c$ = F/T) that limits this

structure only to relatively low-speed applications. Another drawback of this receiver is the strong power loss in optical splitters as the original pulse is divided into k parts at the encoder, then into N_{max} parts at the star coupler, and again to k parts at the optical detector. Therefore, the power of the external modulator pulse will be divided into $N_{max}\,k^2$ parts to form the power of each chip pulse at the receiver.

3. BER PERORMANCE ANALYSIS

In this analysis we assume that different signals are frame asynchronous (no effort has been made to synchronize different transmitters). Analysis of BER of such a system seems to be quite intractable. A simplifying assumption is to consider different signals to be chip synchronous. This is a pessimistic case and gives an upper bound to the BER of the real asynchronous system [2].

In the analysis follows, we have neglected the effect of dispersion on the interference. This assumption is true since the allowable spreading of any chip is only 70% of the chip duration [14]. Also we have used an OOC with a code length that is much greater than the code weight which means that the probability that pulses of users are adjacent to each other is very small [2].

In the passive correlator receiver the BER depends on the number of interfering users n_I only not on the specific interference pattern or the specific users who have produced that pattern [8]. Assuming N-1 interfering users, the BER can be expressed as

$$BER = \sum_{n_I=0}^{N-1} P_r(n_I) P_E(n_I) \qquad (1)$$

where $P_r(n_I)$ is the probability that there are n_I interfering users and is given by

$$P_r(n_I) = \binom{N-1}{n_I} q^{n_I} (1-q)^{N-1-n_I}$$

$$n_I = 0,1,\ldots,N-1. \qquad (2)$$

where q is the probability that two code words overlap in one bit ($q = k^2/2F$) and $P_E(n_I)$ is the probability of error given n_I interfering users and can be expressed as

$$\begin{aligned} P_E(n_I) &= \frac{1}{2} P_E(n_I \mid 0) + \frac{1}{2} P_E(n_I \mid 1) \\ &= \frac{1}{2} \int_{V_{Th}}^{\infty} P_{v_I}(v \mid 0, n_I) dv \qquad (3) \\ &\quad + \frac{1}{2} \int_{-\infty}^{V_{Th}} P_{v_I}(v \mid 1, n_I) dv \end{aligned}$$

where $P_{v_t}(v|b,n_t)$ is the accumulated charge in the integrator which can be modeled as a compound Poisson and Gaussian process since the output of the photodetector is well modeled as a Poisson process [8], and the thermal noise is modeled as a Gaussian process[15]. Hence $P_{v_t}(v|b,n_t)$ can be expressed as

$$P_{v_t}(v|b,n_t) = \sum_{n=0}^{\infty} P(n|b,n_t)\left[\frac{\exp(-(v-e_o n)^2/2\sigma^2)}{\sqrt{2\pi\sigma^2}}\right] \quad (4)$$

where σ^2 is the variance of the output circuit noise of the integrator which is related to the power spectral density N_o (A^2/Hz) by the relation $\sigma^2 = N_o T_c/2$ [8] where T_c is the integration duration, and $P(n|b,n_t)$= Pos (n, M) is the probability of n photoelectron count at the output of the photodetector which can be modeled as a Poisson process with a mean value of $M = ((kb+n_t) M_s + M_d)$. We denote by M_s the mean photoelectron count per chip and by M_d the mean dark current photoelectron count per chip and is given by $M_d = \frac{i_d}{e_o} T_c$, where i_d is the photodetector dark current, and e_o is the charge of an electron. M_s can be expressed as

$$M_S = \eta \frac{E_c}{hf} \quad (5)$$

where f is the operating frequency, h is the Planck's constant, η is the quantum efficiency of the photo-detector, and E_c is the energy of the received chip which depends on the transmitted energy, and the amount of dispersion.

In order to drive an expression for E_c we assume that the output power of the external modulator has a Gaussian shape

$$P_{mod}(t) = P_o \exp\left(\frac{-t^2}{2T_c^2}\right)$$

$$-T_c/2 \le t \le T_c/2 \quad (6)$$

where T_c is the rms value of chip width and P_o is the maximum power of the external modulator. Neglecting the fiber loss, when the dispersion is neglected this pulse will be received at the input to the photodetector with the form

$$P_{ND}(t) = \frac{P_o}{N_{max}\ k^2} \exp\left(\frac{-t^2}{2T_c^2}\right)$$

$$-T_c/2 \le t \le T_c/2 \quad (7)$$

When the dispersion is taken into consideration the maximum amplitude,

and the duration of the received pulses will change. The received pulse at the photodetector can be expressed as

$$P_D(t) = A \quad \exp\left(\frac{-t^2}{2T_{cd}^2}\right).$$

$$-T_{cd}/2 \le t \le T_{cd}/2 \qquad (8)$$

where A is the maximum power of the dispersed chip and T_{cd} is the rms width of the dispersed chip and can be determined as

$$T_{cd} = \left[T_c^2 + \tau_d^2\right]^{1/2} \qquad (9)$$

The value of A can be obtained by equating the energy of the non-dispersed chip to the total energy of the dispersed pulse

$$\text{i.e.} \int_{-T_c/2}^{T_c/2} P_{ND}(t)dt = \int_{-T_{cd}/2}^{T_{cd}/2} P_D(t)dt$$

which will give

$$P_D(t) = \frac{P_o}{N_{max} \quad k^2} \times \frac{T_c}{T_{cd}} \quad \exp\left(\frac{-t^2}{2T_{cd}^2}\right)$$

$$-T_{cd}/2 \le t \le T_{cd}/2 \qquad (10)$$

where τ_d is the rms pulse broadening due to chromatic dispersion which is given by

$$\tau_d = L \ \sigma_\lambda \ |D|. \qquad (11)$$

where L is the fiber length in km, σ_λ is the laser line width in nm, and D_t is the total dispersion parameter in ps/km.nm.

The energy of the dispersed chip E_c can be calculated as follow

$$E_c = \int_{-T_c/2}^{T_c/2} P_D(t) \quad dt =$$

$$\sqrt{2\pi} \quad T_c \quad \frac{P_o}{N_{max} \quad k^2} \quad \text{erf}\left(\frac{T_c}{2\sqrt{2} \quad T_{cd}}\right). \qquad (12)$$

where erf is the error function.

4. NUMERICAL RESULTS

Numerical evaluation of Eq. (3) can be quite time consuming and needs high-precision variables and calculations. Because of the very small values of BER, calculating using ordinary precision variables can make erroneous results. We have used saddle point approximation method [16] in order to compute the numerical value of this integration. This method requires less computation than other standard methods and yield good accuracy. In order to evaluate Eq. (3) using saddle-point approximation method, the moment-generating function (mgf) or the characteristic function of the compound random variable v_t (accumulated charge in the integrator) should be evaluated. The mgf usually

has a mathematical form much simpler than the probability density function (pdf) of the random variable.

In order to apply saddle point approximation method, the Laplace transform of Eq. (3) is taken. As the mgf of the compound random variable v_t is the Laplace transform of the (pdf) of this random variable, then Eq. (3) can be written as

$$P_E(n_1) = \frac{1}{2}\left(L^{-1}\left\{\frac{1-\Phi(s)}{s}\right\} + L^{-1}\left\{\frac{\Phi(s)}{s}\right\}\right)$$
$$= \frac{1}{2}\int_{c-i\infty}^{c+i\infty}\left\{\frac{1-\Phi(s)}{s}\right\}\exp(v_{Th}s)ds/2\pi i + \frac{1}{2}\int_{c-i\infty}^{c+i\infty}\left\{\frac{\Phi(s)}{s}\right\}\exp(v_{Th}s)ds/2\pi i \quad (13)$$

where $\Phi(s)$ is The characteristic function of the compound random variable v_t. By taking the contour in Eq.(13) to the left of the origin, but to the right of all singularities of the mgf $\Phi(s)$, we can write that integral as

$$P_E(n_1) = \frac{-1}{2}\int_{c-i\infty}^{c+i\infty}\left\{\frac{\Phi(s)}{s}\right\}\exp(v_{Th}s)ds/2\pi i + \frac{1}{2}\int_{c-i\infty}^{c+i\infty}\left\{\frac{\Phi(s)}{s}\right\}\exp(v_{Th}s)ds/2\pi i \quad (14)$$

The characteristic function of the compound random variable v_t assuming that the variance of the circuit Gaussian noise is σ^2 and the number of photoelectrons has a Poisson distribution with mean M has been stated in [8] as

$$\Phi(s) = E\left(e^{v_t s}\right) = \exp\left(M\left(e^{c_o s}-1\right)+s^2\sigma^2/2\right) \quad (15)$$

where E standing for the expected value and $M = ((kb+n_1)M_s + M_d)$.

A new function $\psi(s)$ is defined where

$$\psi(s) = \ln\frac{\Phi(s)e^{-v_{Th}.s}}{s} = M\left(e^{c_o s}-1\right)+s^2\sigma^2/2 - v_{Th}.s - \ln|s| \quad (16)$$

where $\frac{\Phi(s)e^{-v_{Th}.s}}{s}$ is the integrand of the integration in Eq.(14).

Positive and negative roots of equation $\psi'(s) = 0$ are called right-hand and left-hand saddle-points and denoted by s_o and s_1 respectively. By expanding the function $\psi(s)$ in Taylor's series about the points s_o and s_1, then using the series expansion of the exponential function exp ($\psi(s)$) and neglecting the higher order terms, the integration in Eq.(14) can be approximated by [16]:

$$\int_{v_{Th}}^{\infty} P_{v_t}(v\,|\,0,n_1)dv \approx \frac{\exp[\psi(s_o)]}{\sqrt{2\pi\psi''(s_o)}} \quad (17)$$

$$\int_{-\infty}^{v_{Th}} P_{v_t}(v\,|\,1,n_1)dv \approx \frac{\exp[\psi(s_1)]}{\sqrt{2\pi\psi''(s_1)}} \quad (18)$$

The equation $\psi'(s) = 0$ must be solved numerically. Because $\psi(s)$ possesses a single minimum in $0 < s < \infty$, Newton's method is most expedient. Starting with a trial value $s_o > 0$, a new trail value is determined by $s_o - \psi'(s_o)/\psi''(s_o)$, and the process is repeated until the values of s_o cease changing significantly. By the same way s_1 can be found, but the initial trail value should be negative. Saddle-point approximation method would be inapplicable, if no left-hand saddle-point exists. Our results showed that Saddle-point approximation method is applicable for all realistic system parameters.

We assume an OCDMA system with the parameters listed in table 1. We have considered three different fiber configurations; the most prevalent fiber type, normal SMF with D_t = 17 ps/km.nm, DSF with D_t = 3 ps/km.nm, and a fully DCF, at λ = 1.55 μm [17]. These types of fiber have been widely deployed in a variety of communications networks worldwide because they are commercially available. The results of BER in each condition have been derived for an optimum threshold value. The BER has been determined for a range of threshold values. An optimum threshold value will result in a minimum BER.

Table1. Used parameters for a proposed FO-CDMA system.

Parameter	Symbol	Assumption
The wavelength	λ	1.55μm
The maximum number of users	N_{max}	27 users
The minimum code length	F_{min}	2000
The code weight	K	9
The photodetector quantum efficiency	η	0.8
The photodetector dark current	i_d	160nA
The noise power spectral density	N_o	$9*10^{-24}A^2/Hz$
The maximum fiber length	L_{max}	150 km

The curves of the mean photoelectron count per chip M_s received at different fiber length for the three configurations; SMF, DSF, and DCF are shown in Fig.3. It is clear from this Figure that as the fiber length increases, the received energy decreases because increasing the length increases the pulse broadening due to chromatic dispersion. The effect of increasing the

fiber length is more apparent in the case of SMF than DSF.

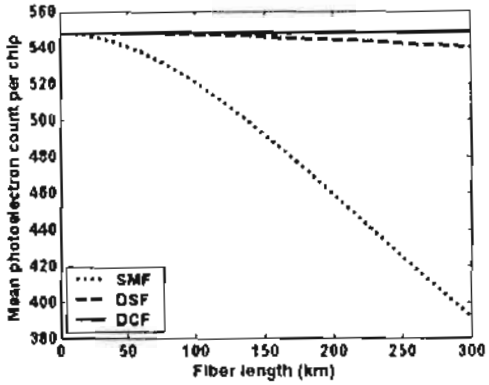

Fig.3. Dependence of the mean photoelectron count per chip on the fiber length, R = 100, Mbps, F =2000, k = 9, σ_λ=0.001nm, and P_o = 40mW.

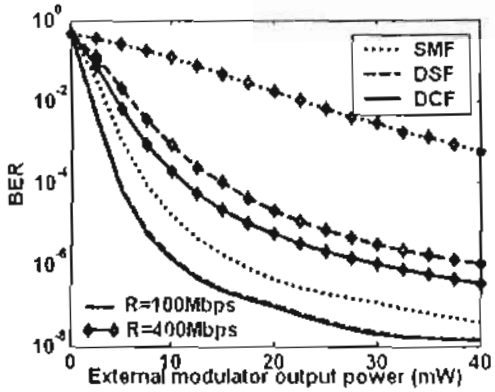

Fig.4. Dependence of BER on external modulator output power, R = 100, 400 Mbps, F =2000, k = 9, σ_λ=0.001, and L = 150km.

The dependence of BER on the external modulator output power P_o for the three configurations; SMF, DSF, and DCF is shown in Fig.4. Two different values of the bit rate; 100 and 400 Mbps have been assumed. The performance of the system is enhanced by increasing P_o but it must be noted that the maximum power lunched on the fiber which is given by

$$(P_{max} = \frac{N_{max}\ P_o}{k} = \frac{27 \times P_o}{9} = 3P_o)$$

exceeds Stimulated Brillouin Scattering (SBS) threshold which is close to 1 mW [17]. This threshold value depends on many parameters; fiber core diameter, fiber attenuation, laser bandwidth, and the wavelength [17]. Hence, SBS threshold will depends on the fiber type that used in the system. In all cases, the used power is relatively high and the effect of SBS must be suppressed as mentioned in the introduction. The results showed also that DSF and DCF configurations perform better than that using SMF. As R_b increases from 100 Mbps to 400Mbps the performance is going worst. This may be explained as follows; the chip duration decreases so, the mean photoelectron count per chip M_s will be reduced, consequently the performance is reduced. On the other hand, the accumulation of noise will decrease for passive correlation receiver which uses a chip time

integrator. However, the reduction in M_s is superior to the reduction in the noises due to their different relations with T_c. It is clear from Fig.4. that the effect of increasing R_b is more apparent in the case of SMF than in the other two cases.

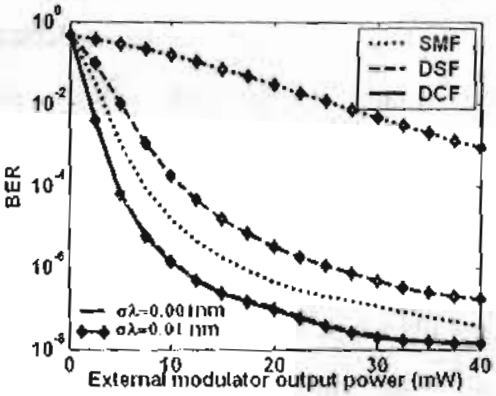

Fig.5. Dependence of BER on external modulator output power, R = 100 Mbps, F =2000, k = 9, σ_λ=0.001, 0.01nm, and L = 150km.

The dependence of BER on the external modulator output power P_o for the three configurations; SMF, DSF, and DCF is shown in Fig.5. for two different values of the spectral line width σ_λ of the LD source; 0.001nm and 0.01nm. Increasing σ_λ increases pulse broadening due to chromatic dispersion which increases the power penalty. This degrades the performance when using SMF and DSF also but in unapparent manner whereas the increasing of σ_λ has no effect on the performance when DCF is used.

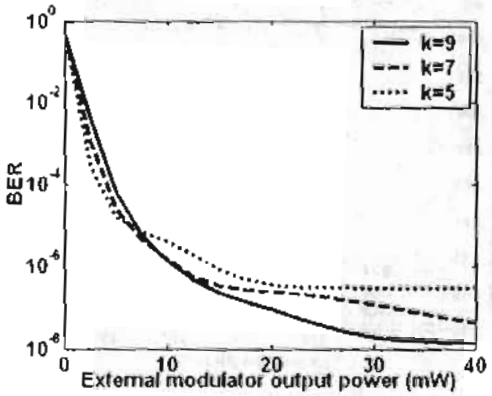

Fig.6.a Dependence of BER on external modulator output power for DCF, R = 100 Mbps, L= 150km, F =2000, and σ_λ=0.001nm, for different values of k.

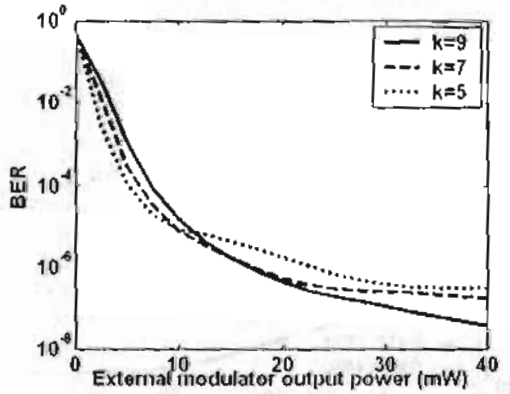

Fig.6.b Dependence of BER on external modulator output power for SMF, R = 100 Mbps, F =2000, σλ=0.001nm, and L = 150km, for different values of k.

For the case of code length F=2000, and maximum number of allowed users N_{max} = 27, the maximum value of code weight k is 9 since the maximum number of users is determined by N_{max} = (F-1)/k (k-1) [12]. The dependence of BER on the

external modulator output power P_o for the DCF and SMF is shown in Fig.6.a and b respectively for different values of k. As k increases, the probability that two code words overlap in one bit q will increase, but it becomes less probable that multiple users will occupy the k mark positions of the intended user and hence the performance improves. However, since the passive correlator receiver is used, the power of the external modulator pulse will be divided into N_{max} k^2 to form the power of each chip pulse at the receiver. This means that increasing k will decrease the mean photoelectron count per chip M_s which will reduce the performance. The reduction in M_s can be neglected if the power is increased. As a result, increasing k enhances the performance in the two cases when the power is greater than a certain power level only. From Fig.6.a and b it can be shown that this power level is about 7.5mW in the case of using DCF and 12mW when SMF is used. It is clear that this power level increases as the fiber dispersion increases because M_s gets smaller as the fiber dispersion gets higher as it is clear from Eq. (12). We observe that for a given code length F and a certain power level, there is an optimum code weight k where the system achieves the best performance, and this optimum value of k varies with the used fiber configuration. This result is clear in Fig.6.c for the SMF where the arrows point to the optimum value of k where the minimum value of BER is obtained.

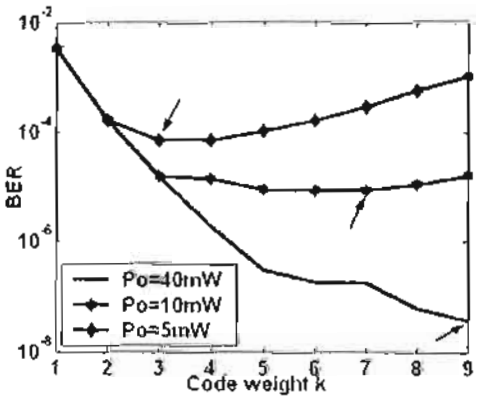

Fig.6.c Dependence of BER on the code weight k for SMF, R = 100 Mbps, F = 2000, σ_λ = 0.001nm, and L = 150km, for different values of external modulator output power.

For the case of N_{max}=27 and k=9, the minimum code length is 2000. The dependence of BER on the external modulator output power P_o for the DCF and SMF is shown in Fig.7.a and b respectively for different values of the code length F.

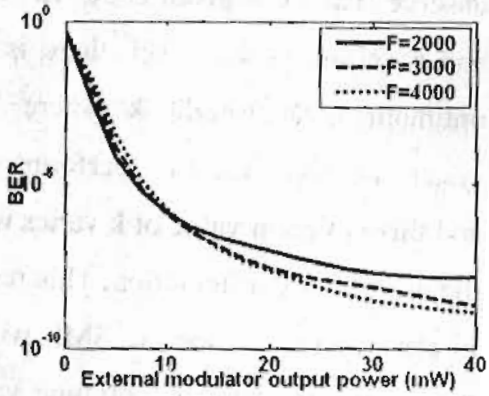

Fig.7.a Dependence of BER on external modulator output power for DCF, R = 100 Mbps, k=9, σ_λ=0.001nm, and L =150km, for different values of F.

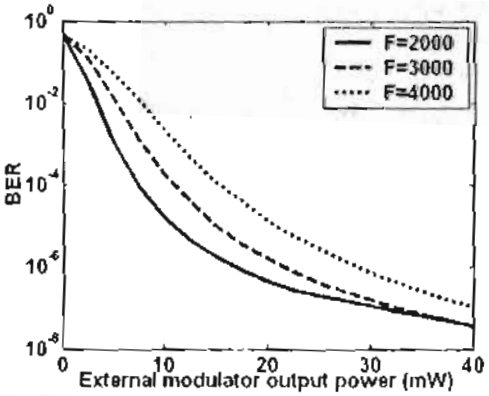

Fig.7.b Dependence of BER on external modulator output power for SMF, R = 100 Mbps, k=9, σ_λ=0.001nm, and L =150km, for different values of F.

As F increases, the probability that two code words overlap q decreases which will enhance the performance. On the other hand, as F increases, the chip duration decreases and hence M_s will decrease also. The reduction in M_s can be cancelled if the power is increased. As a result, increasing F enhances the performance in the case of using DCF when the power is greater than a certain power level only. From Fig.7.a it can be shown that this power level is about 10mW when DCF is used. However, as shown in Fig.7.b, the increase of F degrades the performance in the case of SMF as the power penalty due to dispersion effect is high. Based on the previous results, we observe that for a given code length k and a certain received power level, there is an optimum code length F, where the system achieves the best performance. The optimum value of F varies with the used configuration.

5. CONCULUSIONS

The performance of an OCDMA passive correlator receiver has been analyzed. Optical orthogonal codes (OOCs) are utilized as signature sequences. To our knowledge, a formula for the BER of the system has been developed considering in our calculation, for the first time, the effect of chromatic dispersion. The numerical

results demonstrated that reducing the code weight k enhances the performance when the dispersion is compensated in the system or not at low power only and degrades the performance at high power. In other words, for a given code length F and a certain power level, there is an optimum code weight k where the system achieves the best performance, and this optimum value of k varies with the used fiber configuration.

Finally, the results showed that using an OOC with minimum code length F is the best choice when the SMF is employed in the system. However, when DCF is employed, the minimum code length has to be used at low power levels only which means that for a given code weight k and a certain received power level, there is an optimum code length F, where the system achieves the best performance. The optimum value of F varies with the used configuration.

REFRENCES

1.Xu Wang, and Ken-ichi Kitayama, " Analysis of beat noise in coherent and incoherent time-spreading OCDMA," J. Lightwave Technol., Vol. 22, No.10, pp. 2226-2235, 2004.

2. J. A. Salehi, "Code division multiple access techniques in optical fiber networks-Part I: Fundamental principles", IEEE Trans. Commun., Vol.37, No. 8, pp. 824-833, 1989.

3. Henrik Lundqvist, "Error Correction Coding for Optical CDMA," Laboratory for Communication Networks, Department of Microelectronics and Information Technology, KTH, Royal Institute of Technology, Stockholm Sweden, 2003.

4. Govind P. Agrawal, P. J. Anthony, and T. M. Shen, "Dispersion penalty for 1.3-μm light wave systems with multimod semiconductor Lasers", J. Lightwave Technol., Vol. 6, No.5, pp.620-625, 1988.

5. Eddie K. H. Ng, G. E. Weichenberg, and Edward H. Sargent", Dispersion in multiwavelength optical code division multiple access systems: impact and remedies," IEEE Trans. Commun., Vol. 50, No. 11, pp. 1811-1816, 2002.

6. C. H. Chua, F. M. Abbou, H. T. Chuah, and S. P. Majumder, "Performance analysis on phase-encoded OCDMA communication system in dispersive fiber medium", IEEE Photonics Technol. Lett., Vol. 16, No. 2, pp. 668-670, 2004.

7. J. A. Salehi and C. A. Brackett, "Code division multiple access techniques in optical fiber networks-Part II: System performance analysis", IEEE Trans. Commun., Vol.37, No.8, pp. 834-842, 1989.

8. Sina Zahedi and J. A. Salehi, "Analytical comparison of various fiber optic CDMA receiver structures", J. Lightwave Technol., Vol. 18, No. 12, 2000.

9. Ahmed Elghandour, "Performance analysis of proposed fiber optic receiver structure," Military Technical College, Electrical Engineering Branch, Communication Engineering Department, Cairo, 2004

10. Govind P. Agrawal, " Suppression of stimulated Brillouin scattering in optical fibers using fiber Bragg gratings", Optics Express, Vol. 11, No. 25, pp. 3467-3472, 2003.

11. G.Lenz, B. J. Eggleton, C. K. Madsen, and R. E. Slusher, "Optical delay lines based on optical filters", IEEE J. Quatum Electron., Vol. 37, No.4, pp. 525-532, 2001.

12. Fan R. K. Chung and J. A. Salehi, "Optical orthogonal codes: design, analysis, and applications", IEEE Trans. Inform. Theory, Vol. 35, No. 3, pp. 595-603, 1989.

13. Ivan B. Djordjevic and Bane Vasic, "Novel Combinatorial Constructions of Optical Orthogonal Codes for Incoherent Optical CDMA Systems," J. Lightwave Technol., Vol. 21, No. 9, pp. 1869-1875, 2003.

14. Gerd Keiser, "Optical fiber communications", New York. 1983.

15. B. Saleh, "Photoelectron statistics", Springer-Verlag Berlin Heidelberg New York 1978.

16. C. W. Helstrom, "Approximate evaluation of detection properties in radar and optical communications", IEEE Trans. Aerosp. Electron. Syst., Vol. AES-14, No. 4 pp. 630-640, 1978.

17. John M. Senior, "Optical fiber communications principles and practice", New York. 1985.